

## Research Article

# Research and Implementation of a 1800°C Sapphire Ultrasonic Thermometer

**Haijian Liang,<sup>1</sup> Fengbao Yang,<sup>1</sup> Lu Yang,<sup>1</sup> Zhengguang Liu,<sup>2</sup> Gao Wang,<sup>1</sup> Yanlong Wei,<sup>1</sup> and Hongxin Xue<sup>2</sup>**

<sup>1</sup>National Key Laboratory for Electronic Measurement Technology, North University of China, Taiyuan, Shanxi 030051, China

<sup>2</sup>School of Science, North University of China, Taiyuan, Shanxi 030051, China

Correspondence should be addressed to Fengbao Yang; [yangfengbao1992@163.com](mailto:yangfengbao1992@163.com)

Received 30 May 2017; Revised 30 October 2017; Accepted 5 November 2017; Published 14 December 2017

Academic Editor: Stephane Evoy

Copyright © 2017 Haijian Liang et al. This is an open access article distributed under the Creative Commons Attribution License, which permits unrestricted use, distribution, and reproduction in any medium, provided the original work is properly cited.

A sapphire ultrasonic temperature sensor was produced in this study which possessed working stability, antioxidation properties, and small acoustic-signal attenuation. A method was developed to solve the problems of long periods ( $>0.5$  h) and ultrahigh temperature (1800°C) in tests. The sensor adopted here had good sound transmission performance as well as the high thermal conductivity of sapphire single crystals ( $\text{Al}_2\text{O}_3$ ), as ultrasonic waveguides. The ultrasonic waveguide was produced by the method of the laser-heated pedestal growth (LHPG method). Calibration experiments in a high temperature furnace found that, at high temperatures and long exposure, sapphire ultrasonic temperature sensors had good stability and repeatability, and it survived in 1600°C for 360 min. This sapphire ultrasonic temperature sensor has potential for applications in aircraft engines where monitoring of high temperatures is very important.

## 1. Introduction

Temperature in the nuclear, aerospace, and military industry possesses an important guiding significance, as accurate measurement is important in harsh environments [1], such as in temperature monitoring in nuclear reactors for safe and steady reactor operations [2, 3], temperature tests of aircraft engines to optimize engine design and obtain improved energy efficiency ratios [4], or testing weapon performance in which the temperature is an important measurement index used to assess weapon damage performance [5]. Existing means of measuring temperature mainly include thermoelectric, optical, and acoustical. Thermoelectric temperature sensors as thermocouples have low cost, simple manufacture, and low thermal inertia [6]. However, such thermocouples easily become inaccurate at the hot junction site, which leads to decreased reliability over long use [7]. Thermistor temperature sensors have high output signal, high precision, and low requirements for the secondary instrument, but their disadvantage is a small useful temperature measurement range [8, 9]. Optical temperature sensors include infrared

thermometers and optical fiber temperature sensors. The infrared thermometer measures the temperature distribution without contact [10], which is helpful for testing temperature over a large area and large temperature range. However, when the object emissivity and environmental impact are bigger, test accuracy is decreased [11]. Fiber-optic temperature sensors have high precision, low cost, and distributed multipoints in temperature measurement, and they are not affected by electromagnetic interference. With optical fibers adopted with a silica inner core, high temperatures of 1000°C have been measured [12–14]. The first-order sapphire Bragg gratings were fabricated by Elsmann et al. and the highest temperature at 1200°C [15]. Bragg gratings in single-crystal sapphire optical fibers for high-temperature sensor was fabricated by Busch et al. and they found that at temperatures above 1400°C, the effect of thermal blackbody radiation on the spectrum becomes noticeable. With increasing temperatures, the spectral background signal from thermal radiation collected by air-clad sapphire fibers grows significantly [16]. Sapphire-fiber blackbody-cavity transient high temperature sensors have a 600–1800°C temperature

range [17]. However, radiation below 600°C is small and the low signal-to-noise ratio such that the temperature cannot be effectively measured. Also, when the temperature is greater than 1000°C, stray light into the sapphire fiber poses a problem, as it greatly interferes with accurate temperature measurement and increases measurement errors. Therefore, there is an urgent need for a means of measuring temperature that avoids or solves problems encountered by extreme environment temperature sensors.

Acoustic transmissions of ultrasonic temperature sensors, using acoustics to measure temperature, have wide measurement ranges and are not affected by radiation, with no temperature drift characteristics [18–20], which, for ultra-high temperature measurements, raises hopes for temperature measurement in ultra-high temperature environments. There is an ultrasonic temperature sensor that has been used for high temperature tests in the nuclear industry [21], using tungsten as the sensor material. In this case, the sensor needs an outer protective sheath and is not used directly for rapid temperature measurements [22]. Thus, here, choosing the appropriate sensor material and using ultrasonic temperature measurement methods was expected to solve the problem of temperature measurement in extreme environments. Because of a single sapphire crystal's high melting point, good electrical insulation, and stable chemical performance [16, 23, 24], sapphire waveguide materials became the focus in this study. By combining the advantages of ultrasonic temperature measurement and a sapphire waveguide material, a sapphire was proposed here as an acoustic waveguide ultrasonic thermometer. The device used a laser-heated pedestal for the growth of the ultrasonic waveguide, producing a sensor sensitive from room temperature to 1800°C. The device was calibrated and, with the velocity curve, the ultrasonic sensor tested up to 1800°C.

## 2. Principles

**2.1. The Principle of Ultrasonic Temperature Measurement.** In 1687, Newton discovered the relationship between sound velocity and medium temperature as well as that the velocity of sound in solid medium negatively correlated with temperature. Ultrasonic propagation in material, through the measurement of ultrasonic transit times to calculate sound velocity, and the ambient temperature were obtained according to the relationship of velocity and temperature. Therefore, accurate measurement of the relationship between velocity and temperature has important effects on accurate temperature measurements.

In solid medium, the velocity of ultrasonic longitudinal wave and transverse wave equations can be represented as follows [25]:

$$\begin{aligned} V_L &= \sqrt{\frac{E(1-\sigma)}{\rho(1+\sigma)(1-2\sigma)}}, \\ V_S &= \sqrt{\frac{E}{2\rho(1+\sigma)}}, \end{aligned} \quad (1)$$

with  $V_L$  the longitudinal wave velocity,  $V_S$  the ultrasonic shear wave velocity,  $E$  the elastic modulus of the selected waveguide material,  $\rho$  the material density, and  $\sigma$  Poisson's ratio. The relationship of the ultrasonic longitudinal wave velocity and temperature was chosen for measurement. The sound velocity equation becomes the following formula:

$$V(T) = \sqrt{\frac{E(T)}{\rho(T)}}. \quad (2)$$

When the temperature is  $T$ ,  $V(T)$  is the longitudinal ultrasonic velocity in the waveguide.  $E(T)$  is the elastic modulus and  $\rho(T)$  is the material density at a temperature.

In solids, the relationship of ultrasonic velocity and temperature is usually obtained by an experimental calibration method. When ultrasonic waves are propagated in the waveguide rod, the relationship of the transit time and sound velocity under different temperatures was as follows:

$$t = \int_0^L \frac{1}{v(T)} dx. \quad (3)$$

The length of waveguide rod was  $L$  and  $v(T)$  the speed of sound in the waveguide rod at temperature  $T$ .

In the waveguide rod, the sensitive area was fabricated by the method of mechanical processing (Figure 1). In mechanical processing, 0.2 mm wire with carborundum was used to fabricate the groove in the wire cutting. With the environmental temperature at  $T$  and assuming that the sensitive area length was  $L_1$  and the delay time was  $\Delta t$  the longitudinal ultrasonic wave velocity of the sensitive area was  $V(T)$ . The time of wave packet was  $t$  and two wave packets  $2t$ . The velocity of sapphire at room temperature was  $V_1$ . To distinguish the echoes, the length of sensitive area  $L_1$  was longer than  $2tV_1$ .

$$\Delta t(T) = \frac{2L_1}{V(T)}. \quad (4)$$

**2.2. The Production of a Sapphire Ultrasonic Waveguide Rod.** There are existing sensors made of a variety of materials, such as thorium tungsten or tungsten rhenium alloys. However, materials in the 400–900°C range are prone to oxidation in hostile environments. Such a sensor will be unable to measure the temperature due to oxide osteoporosis in the waveguide rod's surface [26]. Stainless steel has a low melting point (304 stainless steel melting point, 1400°C) and cannot be used in a high-temperature environment. In recent years, sapphire has been widely used in LED semiconductor epitaxial substrates, windows, the dashboards of precision instruments, and high temperature filters [27, 28], having the advantages of high melting point and oxidation resistance. Thus, sapphire was adopted here as the waveguide rod material, but the waveguide rod radius was too small and required thickening. Growth methods for sapphire mainly include edge-defined film-fed growth and laser-heated pedestal method (LHPG) [29–31]. As the LHPG method is the most commonly used method, sapphire optical

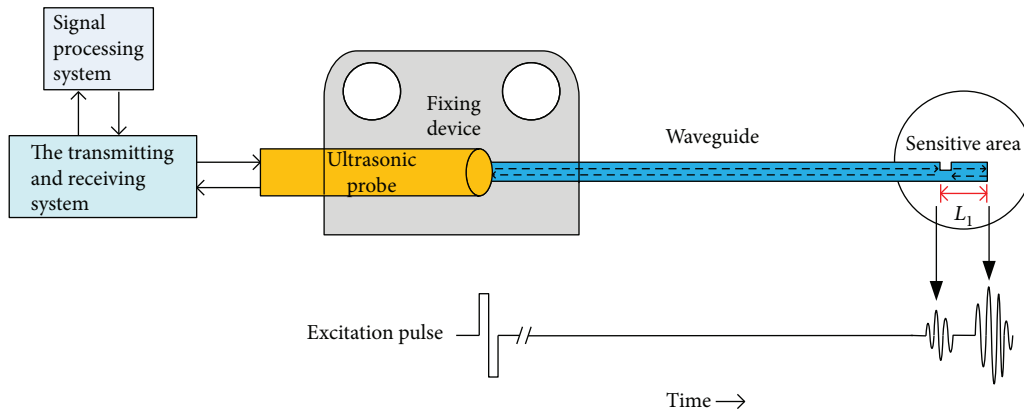


FIGURE 1: The system for ultrasonic temperature measuring.

TABLE 1: The characteristic parameters of sapphire in room temperature (25°C).

Component	Type	Melting point	Mohs hardness	Density	Elastic modulus	Thermal conductivity
$\alpha\text{-Al}_2\text{O}_3$	Single crystal	2053°C	9	3.99 g/cm <sup>3</sup>	310 GPa	0.43 W/cm·K

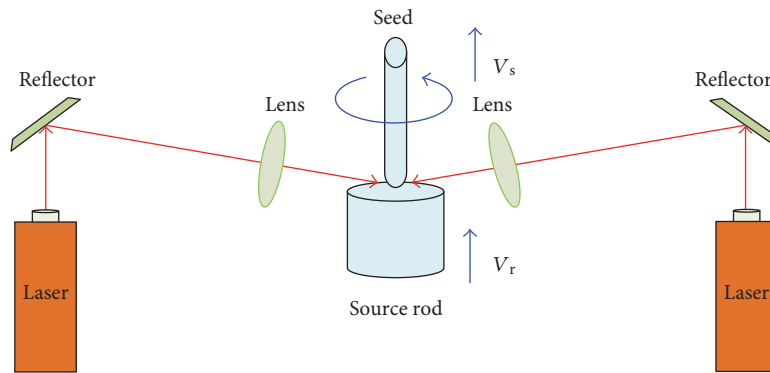


FIGURE 2: The growth apparatus of sapphire.

fibers were grown using the LHPG method and successfully fabricated into a radiation temperature measurement meter by Zhejiang University [32].

Characteristic sapphire parameters are shown in Table 1, showing that the sapphire was a single crystal of  $\text{Al}_2\text{O}_3$  and possessed structural stability, good heat conduction performance, high melting point, and big elastic modulus. Sapphire appeared to be an ideal material for an ultrasonic waveguide for testing at high temperatures and oxidation environments. The sapphire ultrasonic waveguide rods grown here were 99.999%  $\alpha\text{-Al}_2\text{O}_3$ .

The sapphire ultrasonic waveguide was grown by the LHPG method (Figures 2 and 3), using a laser focused on a source rod surface through a reflector and focusing lens, forming a partially melted area on the sapphire. After the seed crystal was uniformly converted into a molten area, the  $V_s$  began to be slowly raised. The source rod was moved upward at a certain speed  $V_r$ , while the source rod and seed crystal bar had uniform rotation. To grow the ultrasonic waveguide rod in accordance with requirements,



FIGURE 3: Sapphire waveguide was grown.

the seed speed  $V_s$  with the source rod speed  $V_r$  satisfied the following relation:

$$\frac{V_s}{V_r} = \left(\frac{D_s}{D_r}\right)^2, \quad (5)$$

with  $D_s$  the seed crystal diameter and  $D_r$  the source rod diameter.

**2.3. Contrast of the Sapphire Ultrasound Waveguide Growth.** When parameters were inappropriately set up in the growth

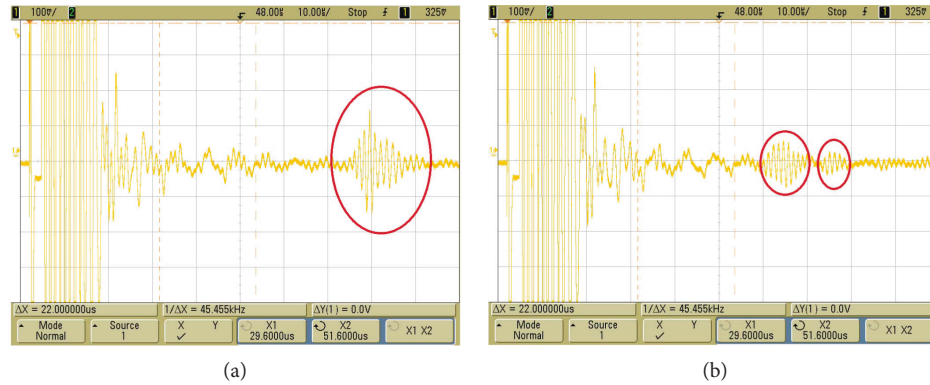


FIGURE 4: Qualified (a) and unqualified (b) contrast waveform.

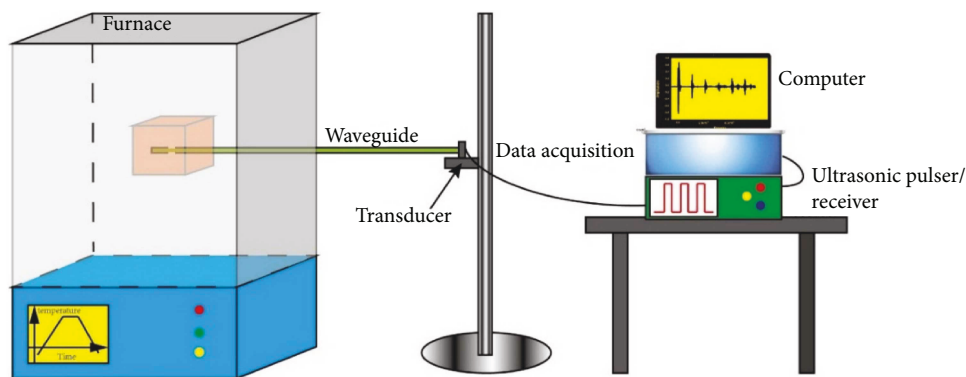


FIGURE 5: Sensor calibration system.

process, an uneven thickness appeared in the ultrasonic waveguide, which was similar to a joint. When the echo characteristics of such a waveguide rod were tested, an echo was found to appear, as with a joint, in the rod. The reason for this was that the diameter of different locations produced echoes, wavelet packets, and small echo amplitude. A qualified waveguide rod was uniform in appearance, with echoes only at the ends and no other stray waves—the end echo signal was larger than in that in unqualified waveguide rods (Figure 4(b)). The formation of uneven thickness was from different growth speeds. In experiments, echoes from uneven thicknesses were not influenced by measurement signals, with the measurement signal covered by it. In the signal processing, the measurement signal could not be extracted.

**2.4. Ultrasonic Temperature Measurement System.** The ultrasonic temperature measurement system is shown in Figure 1, which was composed of a temperature sensing element, ultrasonic transceiver system, A/D collection processing system, and coupling and fixture device. A 340 mm sapphire rod 0.7 mm in diameter was used in experiments. The sensitive area was formed by precision manufacturing technology with the length of the sensitive area at 28 mm. The dispersion phenomenon was effectively avoided when the waveguide diameter was smaller than a quarter of the wavelength. Thus, sapphire waveguides were selected with a diameter of 0.7 mm. At the same time, with a smaller diameter,

thermal equilibrium was reached more rapidly and the response speed greatly improved.

The CTS-8077PR pulse transmitter receiver was adopted in the ultrasonic transceiver system. The ultrasonic transceiver transmitted and received at 2.5 MHz and the A/D acquisition device frequency was 100 MHz. The transit time was calculated by an A/D acquisition device to process the collected sound waves and extract the wave signal. The waveguide rod was coupled in the center of the ultrasonic transducer. The ultrasonic was generated and received by the ultrasonic transducer. When the electrical signal was transmitted and reached the ultrasonic transducer, the ultrasonic wave was generated and entered the waveguide. The ultrasonic wave signal that arrived at the ultrasonic transducer was translated to an electrical signal. The ultrasonic probe and waveguide were fixed in the coupling device, and the waveguide and ultrasonic probe connected with the concentrator.

### 3. Experimental Setup

A temperature resistance furnace was used in the calibration process. The chamber size of the furnace is  $100 \times 100 \times 100$  mm, with the small furnace volume allowing good temperature uniformity. The heat source was provided by heated silicon molybdenum rods and the temperature limit at  $1800^{\circ}\text{C}$  (Figure 5). Measurements were taken at

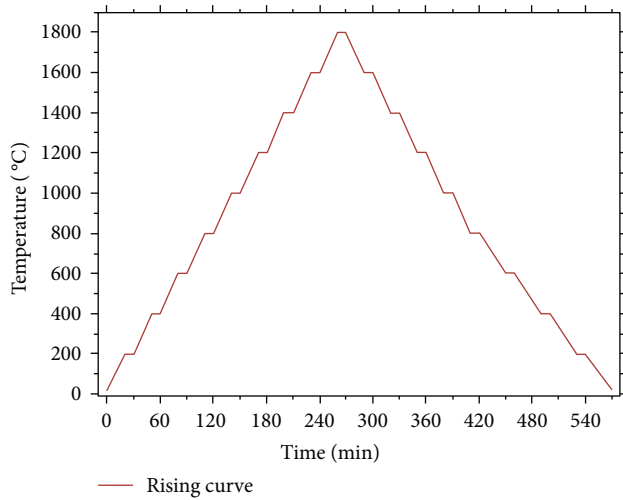


FIGURE 6: High temperature resistance furnace rising-temperature curve.

intervals of 200°C during temperature cycles; starting at room temperature, the temperature was held for 10 min and then returned to room temperature. During the heating process, a platinum rhodium thermocouple with encapsulation was used to record temperature and the platinum rhodium thermocouple temperature at level 2. In experiments, the ultrasonic temperature sensor was placed in the same position as the platinum rhodium thermocouple and the temperature data collected (Figure 6).

As the high temperature furnace's heating limit was 1800 C and it could not be held at this temperature for long periods, after calibration, 1600 C was chosen for stability testing for long periods. In experiments, the temperature was set at 1600 C and data was collected every 20 min up for 360 min, for a total of 19 collection times, and the resulting delay times used to calculate sound velocity and changes in sound velocity.

#### 4. Experimental Results and Analysis

Sapphire was the ultrasonic waveguide material and the experimental temperature cycle from room temperature to 1800°C and back. The characteristic peak was correlated and selected by the algorithm and the delay time was calculated. The experimental results are shown in Figure 7 and the test waveform in Figure 8. In experiments, after several temperature cycles, the relationship between the temperature and delay time was stable, with the delay time deviation at 10 ns. For distinguishing 200 C temperature intervals during rising temperature with a 200 ns transit time, the acquisition card frequency was at 100 MHz, with the acquisition period at 10 ns; the uncertainty was  $\pm 0.01 \mu\text{s}$ . Deviation on the order of nanoseconds was acceptable. The relationship between temperature and delay time was found to have a goodness of fit of  $0.998 \pm 0.001$ . Differences in test results are very small from multiple tests, which indicated that the sensor possessed good repeatability of temperature measurements. With increased temperature, the waveform amplitude showed no obvious attenuation. These results

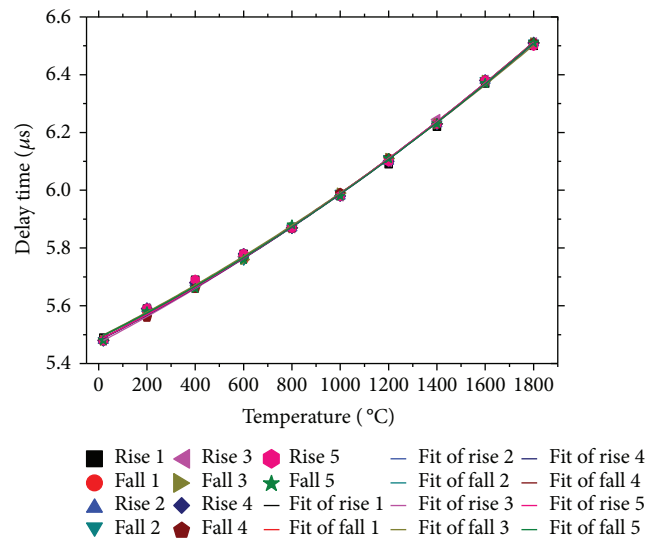


FIGURE 7: Temperature and delay time relationship during temperature cycles.

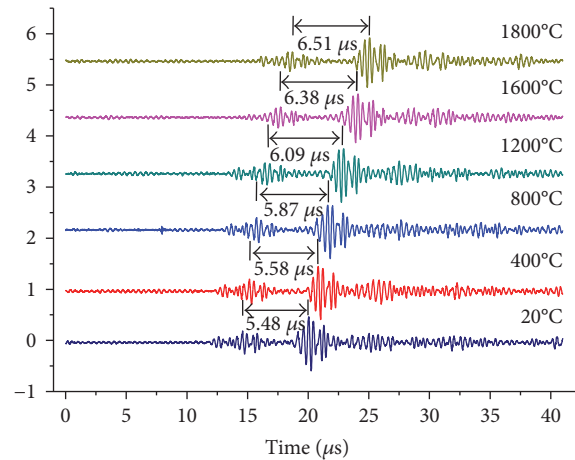


FIGURE 8: The test waveform.

showed that sapphire had little acoustical signal attenuation and that sapphire's structure was stable and its properties showed no obvious changes over this temperature range. Thus, this sensor was very suitable for high temperature measurements.

Using measured delay times and formula (4), sound velocities under different temperatures were calculated. After data fitting, the relationship between velocity and temperature was found to have a goodness of fit of  $0.998 \pm 0.001$  (Figure 9), which indicated that this material was useful from room temperature to 1800 C. When maintained for 360 min at 1600 C, with delay times collected every 20 min, the sound velocity calculated from the delay time was  $8791 \pm 3 \text{ m/s}$  and was found to be stable (Figure 10). Thus, this temperature measuring system, with sapphire as an ultrasonic waveguide, functioned well for long hours in a high temperature environment and exhibited good stability.



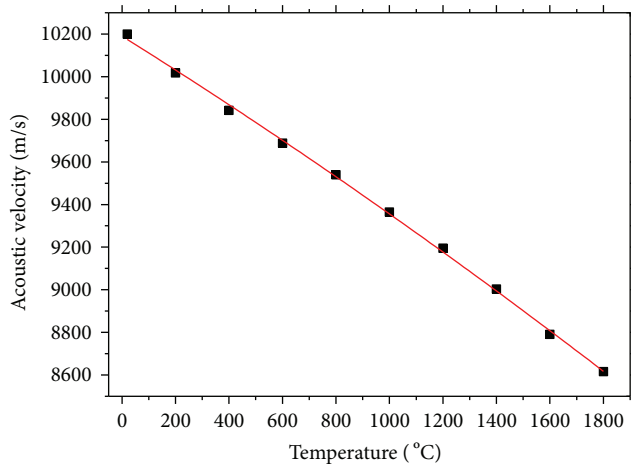


FIGURE 9: Temperature and speed of sound.

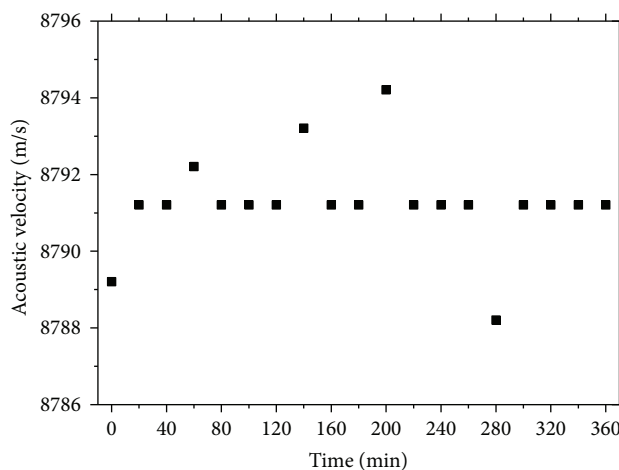


FIGURE 10: Speed of sound over 6 h at 1600°C.

## 5. Conclusion and Prospect

In this paper, a sapphire ultrasonic temperature sensor was designed using the principles of ultrasonic temperature measurement and a sapphire ultrasonic waveguide grown using the LHPG method. The sensor was calibrated from room temperature to 1800°C. During low to high temperature cycling, delay times were measured and the relationship between the delay time and temperature was found to have a goodness of fit of  $0.998 \pm 0.001$ . As a result, this ultrasonic temperature measurement system was found to work well and stably over this temperature range.

Sapphire, as a single crystal material, possesses good sound wave transmission performance, stable structure, and oxidation resistance. The sapphire, as an ultrasonic waveguide, used for temperature measurement avoided accuracy decreases due to material oxidation at high temperatures, thus greatly enhancing system stability. This sapphire ultrasonic temperature sensor solved the problems of the black body cavity of sapphire optical fiber temperature sensors whose lower temperature limit is higher (at 600°C) than room temperature and, also, avoided the influence of stray

light in high temperature measurements. If this sensor is provided a reasonable encapsulation and miniaturization improves detection and the processing equipment, it can be used in aircraft engine performance tests and industrial furnace temperature controls.

## Conflicts of Interest

The authors declare no conflict of interest.

## Acknowledgments

The authors gratefully acknowledge the financial support provided by the National Natural Science Foundation of China (no. 11304289).

## References

- [1] M. J. Holmsten, R. F. Ivarsson, M. Lidbeck, and L. E. Josefson, "Inhomogeneity measurements of long thermocouples using a short movable heating zone," *International Journal of Thermophysics*, vol. 29, no. 3, pp. 915–925, 2008.
- [2] A. H. Antonio, G. M. Rodrigo, and G. M. David, "Drywell temperature prediction of a nuclear powerplant by means of artificial neural networks," *DYNA*, vol. 86, pp. 467–473, 2011.
- [3] H. B. Taehoon and H. C. Seung, "Thin-plate-type embedded ultrasonic transducer based on magnetostriction for the thickness monitoring of the secondary piping system of a nuclear power plant," *Nuclear Engineering and Technology*, vol. 48, pp. 1404–1411, 2016.
- [4] R. Williamson and C. Stanforth, "Measurement of jet engine combustion temperature by the use of thermocouples and gas analysis," *SAE Technical Paper*, vol. 69, p. 19, 1969.
- [5] Y. H. De, M. J. Mutton, J. R. Remiasz, and C. L. Vorres, "Ultrasonic measurements of bore temperature in large caliber guns," *AIP Conference Proceedings*, vol. 28, pp. 1759–1766, 2009.
- [6] A. Mangano and G. Coggiola, "Stability of K-, N- and S-type thermocouples in the temperature range from 0°C to 1060°C," *Measurement*, vol. 12, no. 2, pp. 171–182, 1993.
- [7] J. Chen, X. D. Peng, W. D. Xie, L. J. Feng, A. Z. Zhao, and H. Wang, "Influence of high dose  $\gamma$  irradiation on the calibration characteristics of type K mineral-insulated metal-sheathed thermocouples," *Journal of Alloys and Compounds*, vol. 696, pp. 1046–1052, 2017.
- [8] K. Mitsuteru and T. Katsuhisa, "Thermistor-like PN junction temperature-sensor with variable sensitivity and its combination with a micro-air-bridge heater," *Sensors and Actuators A: Physical*, vol. 108, no. 1–3, pp. 239–243, 2003.
- [9] P. Park, D. Ruffieux, and K. A. Makinwa, "Thermistor-based temperature sensor for a real-time clock with  $\pm 2$  ppm frequency stability," *IEEE Journal of Solid-State Circuits*, vol. 50, no. 7, pp. 1571–1580, 2015.
- [10] J. Manaraa, M. Zipfa, T. Starka et al., "Long wavelength infrared radiation thermometry for non-contact temperature measurements in gas turbines," *Infrared Physics & Technology*, vol. 80, pp. 120–130, 2017.
- [11] Z. Y. Sun, Q. A. Li, Y. F. Qiao, and W. Zhu, "Study on raising the precision of infrared temperature measurement system," *Chinese Journal of Scientific Instrument*, vol. 27, pp. 67–69, 2006.

- [12] L. Liu, Y. Gong, and Y. Wu, "Spatial frequency multiplexing of fiber-optic interferometric refractive index sensors based on graded-index multimode fibers," *Sensors*, vol. 12, no. 12, pp. 12377–12385, 2012.
- [13] T. Stańczyk, K. Wysokiński, and M. Filipowicz, "Electrolytic joints between metal surfaces and metal-coated fibers for application in high temperature optical fiber sensors," *Journal of Lightwave Technology*, vol. 33, no. 12, pp. 2480–2485, 2015.
- [14] P. Xian, G. Y. Feng, and S. H. Zhou, "A compact and stable temperature sensor based on a gourd-shaped microfiber," *IEEE Photonics Technology Letters*, vol. 28, no. 1, pp. 95–98, 2016.
- [15] T. Elsmann, T. Habisreuther, A. Graf, M. Rothhardt, and H. Bartelt, "Inscription of first-order sapphire Bragg gratings using 400 nm femtosecond laser radiation," *Optics Express*, vol. 21, no. 4, pp. 4591–4597, 2013.
- [16] M. Busch, W. Ecke, I. Latka, D. Fischer, R. Willsch, and H. Bartelt, "Inscription and characterization of Bragg gratings in single-crystal sapphire optical fibres for high-temperature sensor applications," *Measurement Science & Technology*, vol. 20, no. 11, article 115301, 2009.
- [17] Y. Q. Guo, W. Xia, and Z. Z. Hu, "High-temperature sensor instrumentation with a thin-film-based sapphire fiber," *Applied Optics*, vol. 56, no. 8, pp. 2068–2073, 2017.
- [18] W. Fan, C. T. A. Chen, and Y. Chen, "Calibration of an acoustic system for measuring 2-D temperature distribution around hydrothermal vents," *Ultrasonics*, vol. 53, no. 4, pp. 897–906, 2013.
- [19] M. Barth and A. Raabe, "Acoustic tomographic imaging of temperature and flow fields in air," *Measurement Science and Technology*, vol. 22, no. 3, article 035102, 2011.
- [20] J. Daw, B. Tittmann, and B. Reinhardt, "Irradiation testing of ultrasonic transducers," *IEEE Transactions on Nuclear Science*, vol. 61, no. 4, pp. 2279–2284, 2014.
- [21] K. M. Koo, D. G. Jeong, J. H. Choi, and D. Y. Ko, "A new measurement system of very high temperature in atomic pile using ultrasonic delay time," in *Proceedings of IEEE Region 10 International Conference on Electrical and Electronic Technology. TENCON 2001 (Cat. No.01CH37239)*, vol. 2, pp. 860–863, Singapore, Singapore, 2001.
- [22] M. Laurie, D. Magallon, and J. Rempe, "Ultrasonic high-temperature sensors: past experiments and prospects for future use," *International Journal of Thermophysics*, vol. 31, no. 8–9, pp. 1417–1427, 2010.
- [23] K. N. Rick and J. A. Harrington, "Optical properties of single-crystal sapphire fibers," *Applied Optics*, vol. 36, no. 24, pp. 5934–5940, 1997.
- [24] P. Capper, *Bulk crystal growth in electronic, optical & optoelectronic materials*, vol. 33, Wiley, German, 2005.
- [25] W. H. Guan, C. Z. Yan, W. H. Chen, and Y. H. Tao, "Ultrasonic shear wave testing under high temperature service environment," *Pressure Vessel Technology*, vol. 21, pp. 4–6, 2004.
- [26] Y. L. Wei, Y. B. Gao, Z. Q. Xiao, and H. J. Liang, "Ultrasonic Al<sub>2</sub>O<sub>3</sub> ceramic thermometry in high temperature oxidation environment," *Sensors*, vol. 16, no. 11, pp. 1905–1915, 2016.
- [27] T. Shimizu and Y. Kogami, "NRD guide excited millimeter wave narrow bandpass filter using sapphire disk resonators," *IEICE Transactions on Electronics*, vol. E95, pp. 1226–1230, 2012.
- [28] J. J. Gagliardia, D. Kima, J. J. Sokola et al., "A case for 2-body material removal in prime LED sapphire substrate lapping and polishing," *Journal of Manufacturing Processes*, vol. 15, no. 3, pp. 348–354, 2013.
- [29] A. V. Denisova, A. Molchanova, Y. O. Puninb, V. M. Krymovc, G. Mullerd, and J. Friedrich, "Analysis of the growth conditions of long single crystalline basal-plane-faceted sapphire ribbons by the Stepanov/EFG technique," *Journal of Crystal Growth*, vol. 344, no. 1, pp. 38–44, 2012.
- [30] C. M. Liu, J. C. Chen, C. H. Chiang, L. J. Hu, and S. P. Lin, "Mg-doped sapphire crystal fibers grown by laser-heated pedestal growth method," *Japanese Journal of Applied Physics*, vol. 45, no. 1A, pp. 194–199, 2006.
- [31] L. D. Iskhakova, V. V. Kashin, S. V. Lavrishchev, Y. Sergey, V. F. Seregin, and V. B. Tsvetkov, "Facet appearance on the lateral face of sapphire single-crystal fibers during LHPG growth," *Crystals*, vol. 6, no. 9, p. 101, 2016.
- [32] L. M. Tong, Y. H. Shen, F. M. Chen, and L. H. Ye, "Plastic bending of sapphire fibers for infrared sensing and power-delivery applications," *Applied Optics*, vol. 39, no. 4, pp. 494–501, 2000.

